A learning rule based on empirically-derived activity-dependent neuromodulation supports operant conditioning in a small network

Article *in* Neural Networks · September 1992

DOI: 10.1016/S0893-6080(05)80140-6 · Source: DBLP

4 authors, including:

Douglas Baxter
University of Texas Health Science Center at …

121 PUBLICATIONS **3,841** CITATIONS

Neural Networks, Vol. 5, pp. 789–803, 1992
Printed in the USA.

0893-6080/92 $5.00 + .00

ORIGINAL CONTRIBUTION

A Learning Rule Based on Empirically-Derived Activity-Dependent Neuromodulation Supports Operant Conditioning in a Small Network

JENNIFER L. RAYMOND, DOUGLAS A. BAXTER, DEAN V. BUONOMANO, AND JOHN H. BYRNE

University of Texas Medical School at Houston

(*Received* 29 *July* 1991; *revised and accepted* 16 *January* 1992)

Abstract—*Activity-dependent neuromodulation has been proposed as a cellular mechanism for classical conditioning in* Aplysia. *Previously, we developed a mathematical model of an* Aplysia *sensory neuron that reflects the subcellular processes underlying this form of associative plasticity. This model could simulate features of nonassociative learning and classical conditioning. In the present study, we tested the hypothesis that activity-dependent neuromodulation could also support operant conditioning. We used a network of six neurons, two of which were adaptive elements with an associative learning rule based on activity-dependent neuromodulation. A two-neuron central pattern generator (CPG) drove the network between two output states. We simulated operant conditioning by delivering reinforcement when one selected output occurred. The network exhibited several features of operant conditioning, including extinction and sensitivity to reversed contingencies, the magnitude of reinforcement, the delay of reinforcement, and contingency.*

Keywords—*Aplysia*, Central pattern generator, Classical conditioning, Learning, Models, Neural networks, Operant conditioning, Plasticity.

1. INTRODUCTION

One of the fundamental problems in neurobiology is to understand events occurring within individual neurons and within networks that contribute to learning and memory. An equally important and related problem is to determine the mechanistic relationships between different forms of learning. For instance, two forms of associative learning that have been studied extensively are classical conditioning and operant (instrumental) conditioning. In classical conditioning, a conditioned stimulus (CS; e.g., a bell), serves as a predictor or signal of the unconditioned stimulus (US; e.g., food), or reinforcement, and thus comes to produce a conditioned response (CR; e.g., salivation) (Pavlov, 1927). In operant conditioning, delivery of the reinforcer (reward or punishment) is contingent on the performance of a particular behavior (the operant) by the animal, and this contingency leads to a change in the frequency of the operant (a decrease in the frequency of a punished behavior or an increase in the frequency of a rewarded behavior) (Skinner, 1938; Thorndike, 1911). Although these two forms of learning have been distinguished in terms of the paradigms that govern the delivery of reinforcement during training, it is not known whether the cellular processes underlying classical conditioning and operant conditioning are fundamentally different or whether these forms of learning may share a common underlying mechanism.

Previous theoretical and empirical work has suggested that at least aspects of classical conditioning and operant conditioning may share a single learning process (Grossberg, 1971; Rescorla, 1987; Tully & Quinn, 1985). The marine mollusc *Aplysia* exhibits both types of associative learning in response systems that are well suited for cellular as well as computational analysis. Therefore, by combining empirical and computational approaches in this system, we hope to gain insight to the mechanisms involved in and the relationship between these two forms of associative learning. Considerable progress has been made in understanding the

Acknowledgments: We thank Mr. S. Patel for assistance with computer programming and graphics. This research was supported by National Science Foundation Fellowship RCD-8851871, Air Force Office of Scientific Research Grant 91-0027, and National Institute of Mental Health Award K02 MH00649 and Fellowship F31 MH09895.

Requests for reprints should be sent to Jennifer L. Raymond, Department of Neurobiology and Anatomy, University of Texas Medical School, P.O. Box 20708, Houston, TX 77225.

neural basis of classical conditioning in *Aplysia* by taking advantage of the simple neural circuitry of two defensive withdrawal reflexes, tail-siphon withdrawal and siphon-gill withdrawal. Using a neural analogue of classical conditioning of these reflexes, a putative cellular mechanism of classical conditioning called activity-dependent neuromodulation has been described. In the neural analogue, activation of a sensory neuron (analogous to the CS) in contiguity with application of a reinforcing stimulus (e.g., stimulation of a nerve, analogous to the US) results in an enhancement of the postsynaptic response (analogous to the CR) that is recorded in a follower neuron (Buonomano & Byrne, 1990; Hawkins, Abrams, Carew, & Kandel, 1983; Walters & Byrne, 1983). The cellular mechanism for activity-dependent neuromodulation appears to emerge from the synergistic action of two intracellular messenger systems, cyclic AMP (cAMP) and Ca^{2+} (for reviews, see Abrams & Kandel, 1988; Byrne, 1985, 1987). The reinforcing stimulus acts via the release of facilitatory transmitter from a facilitatory neuron to increase the intracellular levels of cAMP in the sensory neurons, and, in turn, cAMP produces an enhancement of the synaptic strength of the sensory neurons, expressed when a subsequent test stimulus activates the sensory neuron. The activity dependence (and the associativity) of this form of plasticity results from the ability of Ca^{2+}, which enters a sensory neuron during activity in that neuron, to enhance cAMP production, thereby amplifying the enhancement of synaptic strength in that neuron.

One study of operant conditioning in *Aplysia* has focused on the conditioning of a behavior known as head-waving, during which the animal sweeps its head from side to side to probe its environment (Cook & Carew, 1986, 1989a, 1989b, 1989c). During operant conditioning of this behavior, a reinforcing stimulus is presented whenever the animal waves its head to one side. Following operant conditioning, there is a significant decrease in the amount of time the animals spend head-waving to the punished side compared to their baseline performance (Cook & Carew, 1986). The analysis of conditioning of this behavior is presently being extended to the cellular level (Cook & Carew, 1989a, 1989b, 1989c). However, the location and form of the synaptic plasticity underlying operant conditioning of head-waving are not yet known. Therefore, we have taken a theoretical approach to the question of whether, at the neuronal level, classical conditioning and operant conditioning must involve different mechanisms or whether they could, in fact, result from a single associative plasticity rule. Specifically, we have constructed a computational model containing six neuron-like elements. Two of these elements have properties that reflect activity-dependent neuromodulation, the cellular mechanism that is believed to underlie classical conditioning in *Aplysia*. Previously, the activity-dependent neuromodulation learning rule was mathematically formalized by incorporating equations that describe the biochemical and biophysical mechanisms contributing to this form of plasticity into a detailed model of *Aplysia* sensory neurons (Gingrich & Byrne, 1985, 1987; see Appendix). This model has been able to simulate the neural analogues of several forms of nonassociative learning and of classical conditioning. Furthermore, when elements with this activity-dependent neuromodulation learning rule are incorporated into relatively simple circuits, these networks can simulate some higher-order features of classical conditioning, such as second-order conditioning and blocking (Baxter et al., 1991; Buonomano et al., 1990; Gluck & Thompson, 1987; Hawkins, 1989; Hawkins & Kandel, 1984). In the present study, we examine whether the incorporation of elements with the activity-dependent neuromodulation learning rule into a simple circuit can endow that circuit with the ability to simulate features of operant conditioning. Preliminary reports of these results have been presented (Baxter, Raymond, Buonomano, & Byrne, 1989; Baxter et al., 1991; Byrne, Baxter, Buonomano, & Raymond, 1991).

2. NETWORK ARCHITECTURE

Since the neural circuitry for head-waving and its modulation by operant conditioning are not known, we have constructed a hypothetical neural network that produces an oscillatory pattern similar to head-waving and whose properties are consistent with what is known about invertebrate neurons and networks (Figure 1). The two adaptive elements (AEs) are derived from the single-cell model of Gingrich and Byrne (1985, 1987). The AEs are the only elements of the network whose synaptic strengths can be associatively modified. They are driven by a central pattern generator (CPG), consisting of two spontaneously active and mutually inhibitory neurons (PGs), each of which drives one of the AEs in a spike-to-spike manner. Each AE in turn provides graded excitatory input to a motor neuron (MN), which transforms the input into an activation level. The MNs function as the output of the network, and they also send connections back to the PGs that influence the duration of their bursts. Reinforcement, like the US in simulations of classical conditioning, is modeled as the release of facilitatory transmitter, which causes synthesis of cAMP in the AEs. The reinforcement is diffuse (i.e., it does not selectively affect one or another AE but activates the synthesis of cAMP in both AEs simultaneously). Equations for the AEs and the values of all constants are listed in the Appendix.

2.1. Central Pattern Generator (CPG)

The central pattern generator drives the patterned activity in the network, which serves as the target of op-

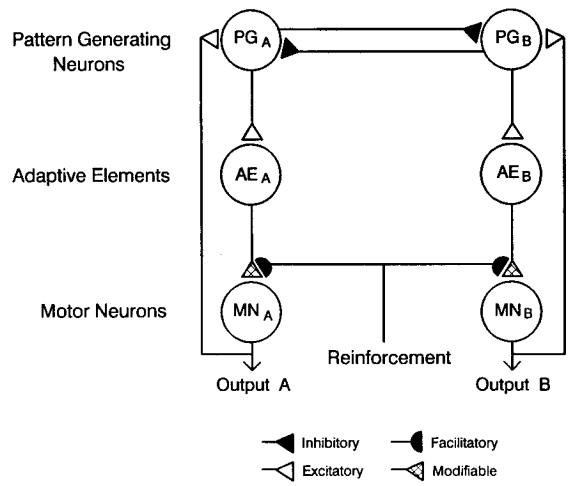

FIGURE 1. Network for simulation of operant conditioning. Two single-cell models incorporating the activity-dependent neuromodulation learning rule have been incorporated into an oscillatory circuit with two possible outputs, A and B. We refer to them as adaptive elements (AEs), since they are the only elements of the network whose synaptic strengths can be associatively modified. The AEs are driven by a central pattern generator (CPG) that consists of two spontaneously active and mutually inhibitory neurons (PGs). Each PG drives one of the AEs in a spike-to-spike manner. Each AE provides graded excitatory input to a motor neuron (MN), which transforms the input into an activation level. The MNs function as the output elements of the network, and they also send connections back to the CPG, which influence the duration of bursts in the PGs. Reinforcement, like the US in simulations of classical conditioning, causes the release of facilitatory transmitter, which causes the synthesis of cAMP in both AEs.

erant training. Its two identical, spontaneously active, and mutually inhibitory cells (PGs) burst in alternation. These bursts are not constant in duration, but are modulated by feedback from the MNs. Since the output of the PGs is not fixed, the PGs can be said to comprise an "adaptive" pattern generator.

The equations and parameters that describe the CPG have been chosen so that it represents a biologically plausible circuit for biphasic oscillation in an invertebrate nervous system. In particular, we have developed a CPG in which (a) the spike duration and frequency in the PGs is reasonable for an *Aplysia* bursting neuron; (b) spike after-hyperpolarizations and inhibitory synaptic potentials fall within typical ranges for *Aplysia* neurons in terms of amplitude and time constants; and (c) the bursts of spikes in the PGs are similar in duration to the head-waves in *Aplysia*.

2.1.1. *Elements of the CPG (PGs).* Each PG is modeled as a membrane capacitance (C_m) in parallel with four ionic conductances, each connected serially to a battery representing the equilibrium potential for the permeant ion. The equivalent electrical circuit is shown in Figure 2. The current through these conductances controls the membrane potential (V_m) of the PGs at and below the threshold for an action potential (−35 mV) according to the relation:

$$dV_m/dt = -(I_{PG,Ca} + I_{PG,Ca,V} + I_{PG,ahp} + I_{PG,syn})/C_m. \quad (1)$$

When the solution of the above equation yields a value of V_m equal to or more positive than −35 mV in one of the PGs, an action potential is simulated by a 3 msec pulse depolarization to +35 mV. The PGs have a 20 msec refractory period after each action potential, during which another action potential cannot be generated.

$I_{PG,Ca}$ is a tonic depolarizing Ca^{2+} current that underlies spontaneous spike activity in the PGs. This current does not exhibit voltage-dependent activation or inactivation, but it is regulated by intracellular Ca^{2+}. $I_{PG,Ca}$ is described by:

$$I_{PG,Ca} = \bar{G}_{PG,Ca} \cdot A_{PG,Ca} \cdot (V_m - E_{Ca}), \quad (2)$$

where $\bar{G}_{PG,Ca}$ is the maximum conductance, E_{Ca} is the equilibrium potential for Ca^{2+}, and $A_{PG,Ca}$ is a decreasing sigmoidal function of the intracellular Ca^{2+} concentration ($C_{PG,Ca}$; See eqn (13)),

$$A_{PG,Ca} = 1 - 1/(1 + \exp(21.0 - C_{PG,Ca})). \quad (3)$$

Since $I_{PG,Ca}$ contributes directly to the accumulation of Ca^{2+} (see eqn (13)), it contributes to its own inactivation. Inactivation of $I_{PG,Ca}$ in turn causes an increase in the interspike interval and ultimately termination of the burst (see below). Such Ca^{2+}-dependent inactivation of a Ca^{2+} current has been described in neurons of *Aplysia* (Eckert & Tillotson, 1981; Kramer & Zucker, 1985) and other invertebrates (e.g., *Helix*, Oyama, Akaike, & Nishi, 1986). Furthermore, CPGs containing mutually inhibitory cells have been described in a number of invertebrates (Calabrese & Peterson, 1983; Getting, 1981, 1989; Selverston, Miller, & Wadepuhl, 1983).

A voltage-dependent K^+ current, $I_{PG,ahp}$, is responsible for the spike after-hyperpolarization in the PGs.

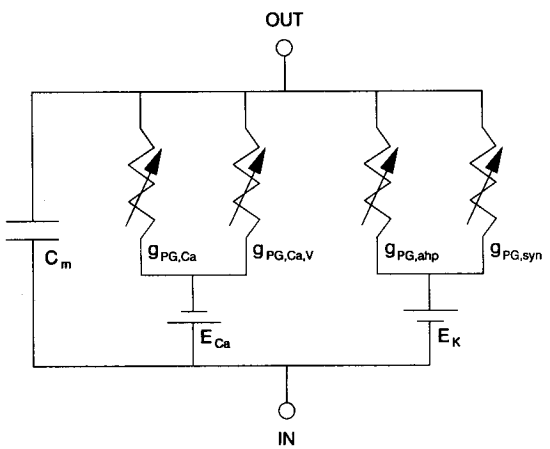

FIGURE 2. Equivalent circuit for PGs. The four membrane conductances of the PGs are modeled as parallel conductances, each in series with a battery that represents the equilibrium potential for the ion that carries the current. The conductances are also in parallel with a membrane capacitance.

Since it tends to oppose $I_{PG,Ca}$, it also contributes to the interspike interval. The equation describing $I_{PG,ahp}$ is

$$I_{PG,ahp} = \bar{G}_{PG,ahp} \cdot A_{PG,ahp} \cdot (V_m - E_K), \quad (4)$$

where $\bar{G}_{PG,ahp}$ is the maximum conductance, $A_{PG,ahp}$ represents voltage-dependent activation, and E_K is the equilibrium potential for K^+. During a spike in a neuron of the pattern generator,

$$A_{PG,ahp} = 1 - \exp(-t_1/T_{PG,ahp}), \quad (5)$$

in that neuron, where t_1 is the time from the beginning of the pulse depolarization (spike) and $T_{PG,ahp}$ is the time constant for voltage-dependent activation. Between spikes

$$A_{PG,ahp} = A'_{PG,ahp} \cdot \exp(-t_2/T_{PG,ahp}), \quad (6)$$

where $A'_{PG,ahp}$ is the value of $A_{PG,ahp}$ at the end of the last spike and t_2 is the time since the end of that spike.

A second Ca^{2+} current, $I_{PG,Ca,V}$, is a voltage-dependent Ca^{2+} current. Its voltage-dependent activation ($A_{PG,Ca,V}$) is described by equations similar to eqns (5 and 6). The maximum conductance ($\bar{G}_{PG,Ca,V}$) of $I_{PG,Ca,V}$ is larger than that of the voltage-independent current $I_{PG,Ca}$. $I_{PG,Ca,V}$ can therefore contribute significantly to the accumulation of Ca^{2+} despite its small time constant ($T_{PG,Ca,V}$), which causes it to be active only briefly in response to a spike. This conductance thus contributes to the termination of a burst through the Ca^{2+}-dependent inactivation of $I_{PG,Ca}$.

$I_{PG,Ca,V}$ is also the conductance through which feedback from the MNs acts on the CPG. A MN modulates $I_{PG,Ca,V}$ in the ipsilateral PG, and thus affects the rate of Ca^{2+} accumulation and ultimately burst duration in that PG. Activity in a MN (*AMN*; see below) produces feedback (F) according to the relation

$$dF/dt = (AMN - F)/T_{FB}, \quad (7)$$

where T_{FB} is the time constant for feedback. The modulation (M) of $I_{PG,Ca,V}$ by this feedback is described by

$$M = 1 - (K_{FB} \cdot F), \quad (8)$$

where K_{FB} is a constant and $0 \leq F \leq 1$, so that

$$I_{PG,Ca,V} = \bar{G}_{PG,Ca,V} \cdot A_{PG,Ca,V} \cdot M \cdot (V_m - E_{Ca}). \quad (9)$$

As *AMN* increases, F increases, M decreases, and the amount of Ca^{2+} that accumulates with each spike is reduced. Thus, it takes longer for Ca^{2+} to build up to the point at which it inactivates $I_{PG,Ca}$ enough to terminate the burst (see below). The result is that an increase in the strength of an AE-to-MN synapse leads to an increase in the duration of the bursts of activity on that side of the network.

The synaptic current, $I_{PG,syn}$, is a potassium current. It mediates the mutual inhibition between the two cells of the CPG that causes one cell to be silent while the other is firing. It is activated in one PG by the occurrence of a spike in the other PG; in essence, this current results in inhibitory postsynaptic potentials (IPSPs) from the spiking cell onto the other cell in the CPG. Thus,

$$I_{PG,syn} = \bar{G}_{PG,syn} \cdot A_{PG,syn} \cdot (V_m - E_K), \quad (10)$$

where $\bar{G}_{PG,syn}$ is the maximum conductance, and $A_{PG,syn}$, the activation of $I_{PG,syn}$ in a PG is described by

$$A_{PG,syn} = 1 - \exp(-t_1/T_{PG,syn}), \quad (11)$$

when the other PG initiates a spike, and by

$$A_{PG,syn} = A'_{PG,syn} \cdot \exp(-t_2/T_{PG,syn}), \quad (12)$$

when the other PG is not firing a spike. (t_1 is the time from the beginning of a simulated action potential in the contralateral PG; t_2 is the time since the end of the last spike in the contralateral PG; and $A'_{PG,syn}$ is the value of $A_{PG,syn}$ at the end of that spike.)

The PGs also contain equations that describe the regulation of Ca^{2+}, which includes both passive diffusion ($F_{PG,DC}$) and active uptake ($F_{PG,UC}$) from the cytosol into compartments of the PG that are not modeled. Thus,

$$dC_{PG,Ca}/dt = (I_{Ca,in} - F_{PG,UC} - F_{PG,DC})/V_{PG}, \quad (13)$$

where

$$F_{PG,DC} = K_{PG,DC} \cdot C_{PG,Ca} \quad (14)$$

$$F_{PG,UC} = K_{PG,UC}/(1 + \exp(1.0 - C_{PG,Ca})), \quad (15)$$

$I_{Ca,in}$ is the combined Ca^{2+} influx through $I_{PG,Ca}$ and $I_{PG,Ca,V}$, V_{PG} is the volume of the cytosol in the PG, and $K_{PG,DC}$ and $K_{PG,UC}$ are the constants for diffusion and uptake, respectively. $F_{PG,DC}$ and $F_{PG,UC}$ oppose accumulation of Ca^{2+} while the cell is bursting and cause a return of the Ca^{2+} concentration towards baseline when the cell is silent. Hence, Ca^{2+} buffering allows recovery of $I_{PG,Ca}$ from Ca^{2+}-dependent inactivation.

2.1.2. *Production of Patterned Network Activity.* The interaction of the four conductances and the Ca^{2+} regulation system yields a bursting behavior as follows: A burst of action potentials in one PG (e.g., PG_A) produces summating IPSPs in the contralateral PG. Due to this inhibition, the contralateral PG is silent (Figure 3). Therefore, there are no IPSPs in the cell that is firing, $I_{PG,Ca}$ in that cell is opposed only by $I_{PG,ahp}$, and hence it continues to fire. As it fires, however, Ca^{2+} accumulates within the cell. This accumulation of Ca^{2+} causes inactivation of $I_{PG,Ca}$. With less depolarizing current to oppose $I_{PG,ahp}$, the cell reaches threshold more slowly with each spike, and the spike frequency decreases (Figure 4). In the contralateral cell, the frequency of the IPSPs decreases, allowing the membrane potential of that cell to recover towards threshold and eventually fire. At this point, both cells are near threshold, but because of Ca^{2+}-dependent inactivation, the cell that had been firing has a much smaller $I_{PG,Ca}$ with which to oppose $I_{PG,ahp}$ and the new hyperpolarizing

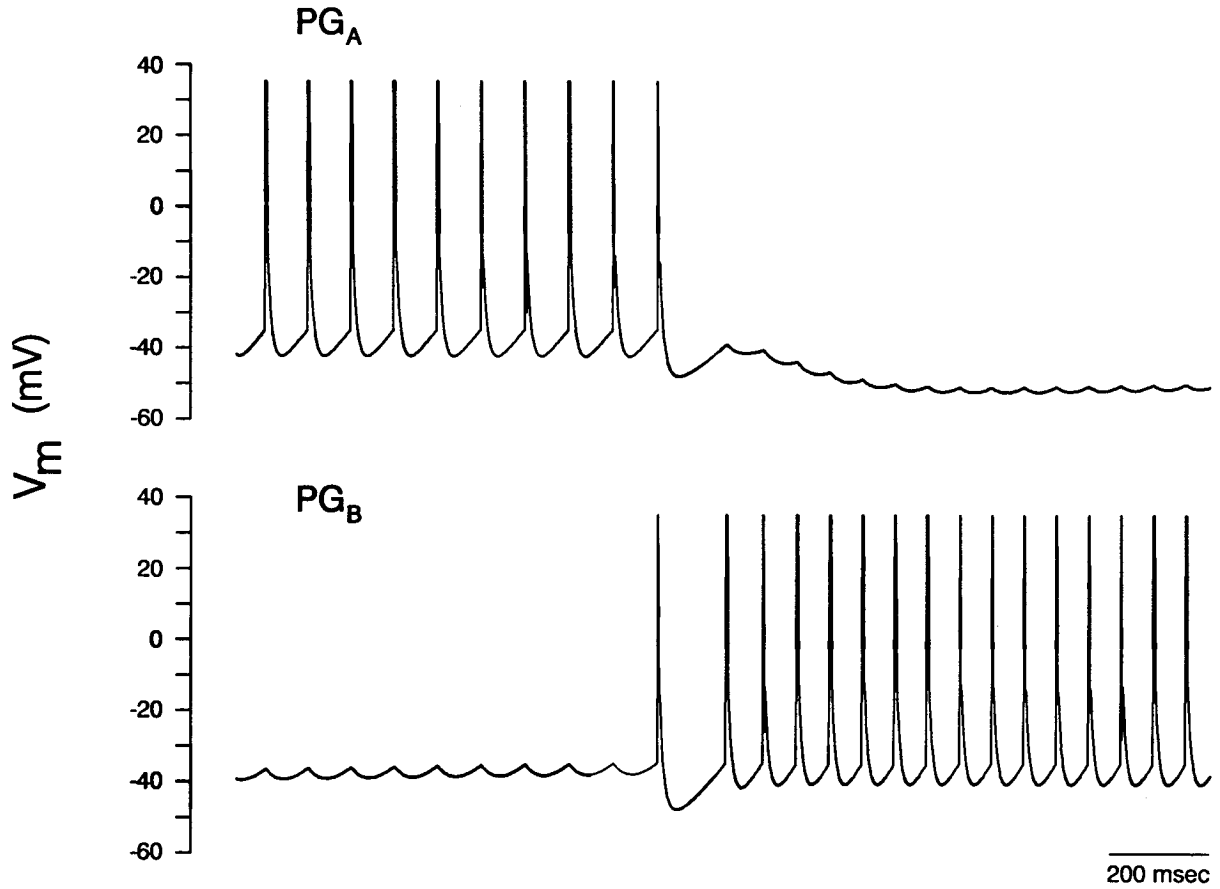

FIGURE 3. Bursting pattern in the CPG. The membrane potential (V_m) of each PG is controlled by four membrane conductances. Action potentials are simulated by a 3 msec pulse depolarization to +35 mV that is triggered when V_m reaches a threshold of −35 mV. Spikes in PG_A activate a synaptic current that produces IPSPs in PG_B. As the frequency of the IPSPs declines, PG_B reaches threshold and begins to spike, producing IPSPs in PG_A.

contribution of $I_{PG,syn}$, so it is hyperpolarized while the previously silent cell continues to fire. During the burst in the contralateral cell, buffering causes the Ca^{2+} level in the first cell to recover towards baseline, allowing the recovery of $I_{PG,Ca}$ from Ca^{2+}-dependent inactivation. The first cell can then begin firing when the spike frequency in the contralateral cell declines.

Thus, oscillation of the CPG depends on the mutual inhibition of the two PGs and the gradual release from inhibition that occurs in one PG as the spike frequency decreases in the other PG as the result of Ca^{2+}-dependent inactivation of a Ca^{2+} conductance. If the inhibitory synapses were removed from the circuit, both PGs would fire continuously at a constant, low frequency (not shown).

2.2. Adaptive Elements (AEs)

The PGs drive the AEs in a spike-to-spike manner. The AEs are the elements of the network into which activity-dependent neuromodulation was incorporated. The detailed model of *Aplysia* sensory neurons (Gingrich & Byrne, 1985, 1987) contains descriptions of the biochemical and biophysical mechanisms contributing to this form of plasticity. It includes differential equations describing two pools of transmitter, a releasable pool and a storage pool. Vesicles of transmitter are mobilized from the storage pool to the releasable pool via three fluxes, one driven by diffusion, one driven by Ca^{2+}, and one driven by cAMP. There are also equations describing the regulation of the intracellular levels of Ca^{2+} and cAMP. Action potentials lead to an influx of Ca^{2+}, Ca^{2+} accumulation, and release of transmitter. Facilitatory transmitter leads to the synthesis of cAMP, which in turn leads to the mobilization of transmitter and an increase in the duration of action potentials, thus allowing for greater Ca^{2+} influx and enhanced transmitter release. When a burst of action potentials precedes the application of the facilitatory transmitter, the elevated level of intracellular Ca^{2+} amplifies the synthesis of cAMP. The equations and parameters of this model are detailed in the Appendix.

Among other synaptic phenomena, the original single-cell model simulated synaptic depression (Gingrich & Byrne, 1985). The present simulations required that the AEs simulate activity-dependent neuromodulation but not undergo extreme depression during high-frequency spiking lasting tens of seconds. All equations

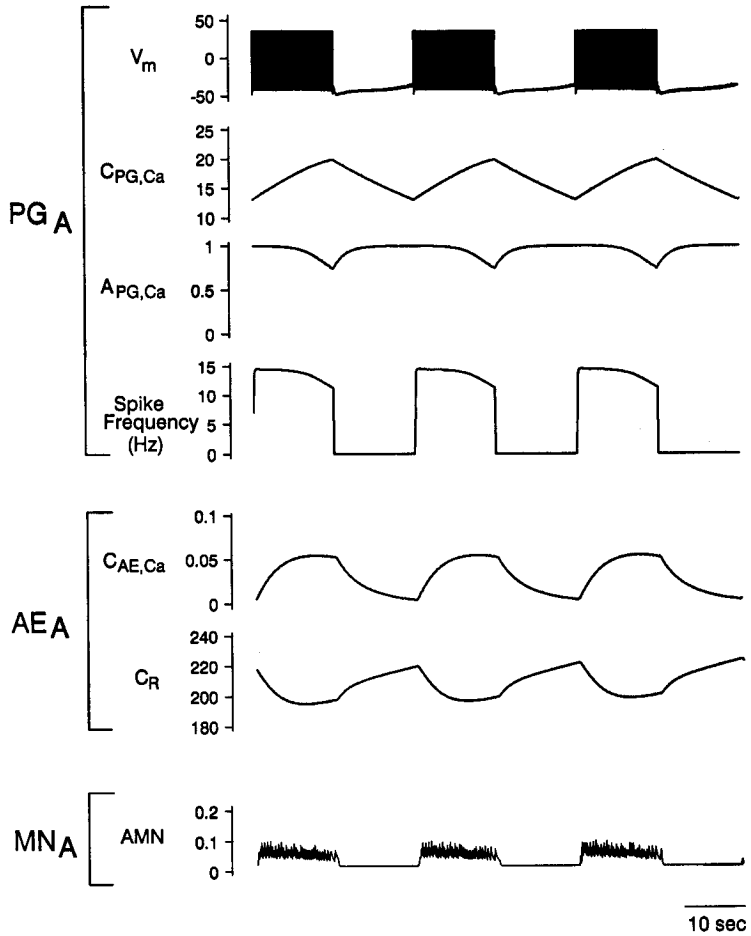

FIGURE 4. Behavior of key components of the network before training. Records are from elements on one side of the network during the baseline period. Pattern Generating Neuron (PG_A): A voltage-independent Ca^{2+} current ($I_{PG,Ca}$) in each PG provides tonic depolarizing current that underlies the spontaneous spike activity in the CPG. Its activation level is represented by $A_{PG,Ca}$. During a burst of spikes in PG_A, the concentration of Ca^{2+} ($C_{PG,Ca}$) increases, and Ca^{2+}-dependent inactivation of $I_{PG,Ca}$ causes the spike frequency to decrease. Eventually, PG_B (not shown) fires, inhibiting PG_A and terminating its burst. During the burst in PG_B, PG_A is silent, and Ca^{2+} in PG_A is buffered, removing the inactivation of $I_{PG,Ca}$. Adaptive Elements (AEs): A burst of activity in PG_A causes spiking and the accumulation of Ca^{2+} ($C_{AE,Ca}$) in AE_A. When the AE is silent, there is no Ca^{2+} influx, and the Ca^{2+} that accumulated during the previous burst is buffered. While the AE is spiking, mobilization of transmitter cannot keep up with release, and depletion of the releasable pool of transmitter (C_R) occurs, but when the AE is silent, mobilization replenishes C_R. The slight increase in C_R towards the end of a burst reflects Ca^{2+}-dependent mobilization of transmitter. Motor Neurons (MNs): Release of transmitter from an AE causes activation of the ipsilateral MN (*AMN*), which serves as the output of the network and provides feedback to the ipsilateral PG.

and parameters for the AEs are therefore as described in Gingrich and Byrne (1985, 1987; see Appendix also) for the single-neuron model with the exception of the following changes, which were made to compensate for the increased activity levels in the present simulations. These changes did not alter the ability of the model to support classical conditioning.

First, the time constant for recovery of the voltage-dependent Ca^{2+} current ($I_{AE,Ca}$) from inactivation was reduced. This allows the AEs to burst for several seconds while maintaining $I_{AE,Ca}$ at a level that supports continued transmitter release. Second, depletion of transmitter from the releasable pool was reduced by increasing the pool size, by eliminating depletion of the storage pool, and by reducing the amount of transmitter released with each spike. The storage pool was maintained by removing its dynamics and setting it to a constant value of 100. The reduction in transmitter release was accomplished by decreasing the gain constant for release (K_R) and by reducing the gain constant for the Ca^{2+} current (K_C). The diffusion constant for Ca^{2+} (K_D) was reduced, and, finally, a saturation level or 'ceiling' (C_{max}) was placed on the intracellular level of cAMP. All of the new constants are listed in the Appendix.

During the oscillatory activity of the network, a burst of activity in one PG (e.g., PG_A) causes spiking and the accumulation of Ca^{2+} in the corresponding AE (AE_A) (Figure 4). When the burst terminates and the AE is silent, there is no Ca^{2+} influx, and the Ca^{2+} that accumulated during the previous burst is buffered. Similarly, while the AE is spiking, mobilization of

transmitter cannot keep up with release, and depletion of the releasable pool (C_R) occurs, but when the AE is silent, mobilization replenishes C_R.

2.3. Motor Neurons (MNs)

The response of the MN membrane (V_{EPSP}) to transmitter (T_R) released from an AE is approximated as an RC circuit:

$$dV_{EPSP}/dt = (T_R - V_{EPSP})/T_M. \quad (16)$$

This membrane response determines the activation level in the motor neuron (AMN) according to the sigmoidal function

$$AMN = 1/(1 + \exp((20.0 - V_{EPSP})/5.0)). \quad (17)$$

AMN, as the output of the motor neurons, can be thought of as either the instantaneous spike frequency of the MNs or as the amount of transmitter being released from the MNs. AMN is the measure of network behavior. The activation of one MN represents the occurrence and strength of one output or behavior while the activation of the contralateral MN represents the occurrence and strength of a competing output or behavior. Through its feedback connections to the CPG, AMN also modulates the oscillatory pattern of the network.

2.4. Reinforcement

Reinforcement is mediated by the release of facilitatory transmitter, which has access to both AEs (Figure 1). Reinforcement causes the synthesis of cAMP in each AE at a rate directly proportional to the concentration of Ca^{2+} in the AE ($C_{AE,Ca}$). Thus, the concentration of cAMP (C_{cAMP}) changes according to the relation

$$dC_{cAMP}/dt = (K_{EC} \cdot C_{AE,Ca}) - C_{cAMP}/T_{cAMP}. \quad (18)$$

K_{EC} is the gain constant for the associative synthesis of cAMP (in the absence of reinforcement, $K_{EC} = 0$), and T_{cAMP} is the time constant for the decay of cAMP. C_{cAMP} has a ceiling, C_{max}.

To allow the modulatory input to act over relatively long periods of time (tens of seconds) without increasing cAMP to extremely high levels, we have reduced the associative gain constant (K_{EC}) used by Gingrich and Byrne (1987) and have removed the K_{SC} term, which represented nonassociative (Ca^{2+}-independent) plasticity. The synthesis of cAMP leads to the facilitation of the synaptic connections between the AEs and their follower neurons, the MNs.

3. SIMULATIONS OF OPERANT CONDITIONING

3.1. Contingent Reinforcement Paradigm

The basic training paradigm consisted of a 400 sec baseline phase and one or more 40 min training phases. During the baseline phase no reinforcement was delivered. During contingent training, activity in one of the MNs was chosen as the reinforced output, and reinforcement was delivered (cAMP synthesis was activated) whenever activity in that MN exceeded activity in the nonreinforced output for at least 0.5 sec.

The result of this procedure is shown in the records of activity in the MNs (Figure 5a). When the delivery of reinforcement was contingent on the occurrence of activity in MN_A, there was an increase in the duration of each burst in MN_A. Although the duration of bursts in MN_B also increased, the increase in MN_A was much greater, and therefore the network spent relatively more time producing the reinforced output, Output A, as a result of contingent training. This result is displayed graphically in Figure 5c. Conditioning is plotted as the difference between the time spent producing Output A and the time spent producing Output B during each cycle of the network, where a cycle is defined as one complete oscillation of the network through an occurrence of each output. During contingent training, a progressively greater amount of time within each cycle was devoted to producing the operant response, Output A.

These results depend upon the interaction of the Ca^{2+} and cAMP pathways in the AEs (Figure 6). During contingent training, reinforcement coincided with activity (and therefore a high concentration of Ca^{2+}) in the AE on the reinforced side of the network (AE_A). Because of the mutual inhibition of the cells of the pattern generator, reinforcement occurred during a time when AE_B was inactive and contained only a small amount of residual Ca^{2+}, which had accumulated during a previous burst and which had not yet been buffered. Since the amount of cAMP (and hence facilitation) that is produced in response to the presence of reinforcement is proportional to the intracellular Ca^{2+} concentration, the reinforcement caused cAMP to be produced in both AEs, but caused much more cAMP to be produced in AE_A. Therefore, the reinforcement produced facilitation of both AE-to-MN synapses, but the AE_A-to-MN_A synapse was facilitated to a much greater degree. The releasable pool of transmitter (C_R) became much larger and action potentials became much broader in AE_A than in the baseline condition. Therefore, the same activity in PG_A resulted in more transmitter release from AE_A and stronger activation of MN_A. This meant greater feedback to PG_A, and hence longer bursts of activity on the reinforced side of the network than in the baseline condition. The nonreinforced side of the network, on the other hand, did not manifest changes of such magnitude. With continued training, cAMP in AE_A reached its saturation level (not shown). No further enhancement of the AE_A-to-MN_A synapse occurred, and the duration of bursts of activity on that side of the network stabilized at a duration approximately six times as long as the duration of a burst during baseline.

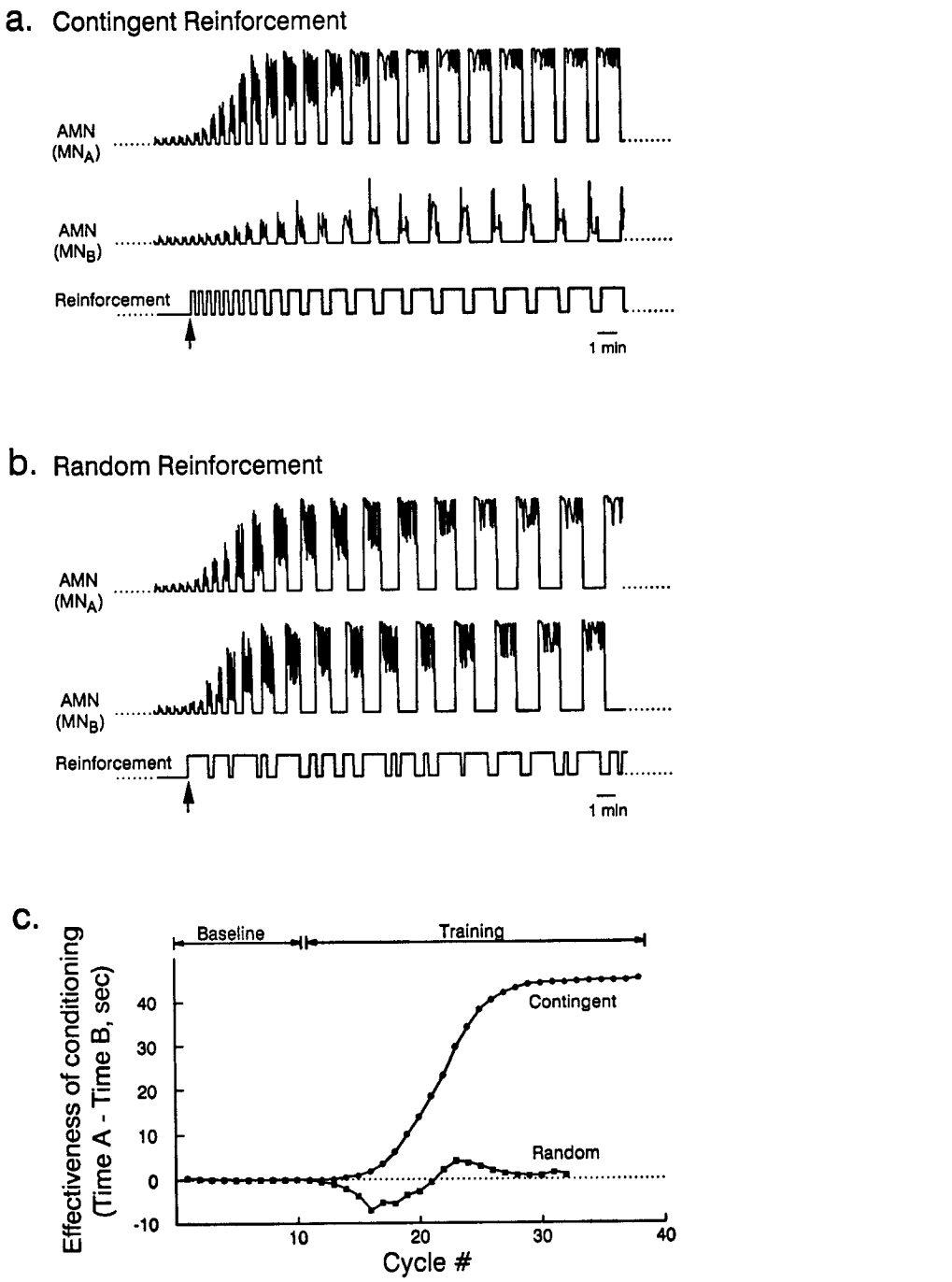

FIGURE 5. Network output during simulations of operant conditioning. (a) Contingent reinforcement. Training begins at the arrow. In this case, Output A is chosen as the reinforced behavior, and reinforcement is delivered whenever MN_A is active. During training, there is an increase in both the amplitude and the duration of bursts of activity in MN_A. Although activity in MN_B also increases, the increase in MN_A is much greater; thus, the network spends relatively more time producing Output A. (b) Random reinforcement. There is an increase in the amplitude and duration of bursts of activity in both MNs; however, the network does not spend more time producing Output A than it spends producing Output B. (c) Results from the simulations in A and B are summarized as the difference between the time spent producing Output A and the time spent producing Output B for each behavioral cycle, where a cycle is one complete oscillation of the network through a burst of activity in each MN.

With the behavioral paradigm that has been used for operant conditioning of head-waving, the reinforced behavior does not completely displace the nonreinforced behavior (Cook & Carew, 1986). Both behaviors continue after training, but the relative amount of time spent producing each behavior changes. Similarly, in the simulations, both outputs continued after training. On the nonreinforced side of the network, the duration of bursts increased due to the small amount of cAMP in AE_B, but the increase was small relative to the rein-

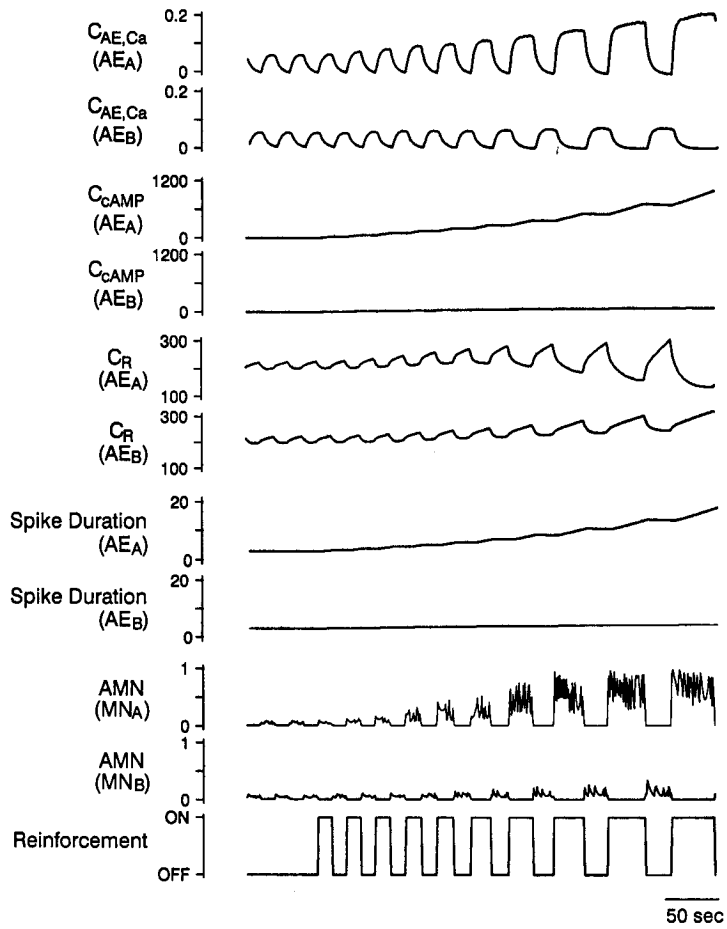

FIGURE 6. Behavior of key components of the network during simulations of operant conditioning. When reinforcement is contingent on the production of Output A, reinforcement coincides with activity (and therefore a high concentration of Ca^{2+}) in AE_A and inactivity (low Ca^{2+}) in AE_B. Therefore, reinforcement causes more cAMP to be produced in AE_A. Consequently, C_R is larger and spikes are broader in AE_A. Therefore, activity in PG_A results in more transmitter release from AE_A, greater activation of MN_A, greater feedback to PG_A, and hence longer bursts of activity on the reinforced side of the network.

forced side. The bursts on the nonreinforced side continued to increase until they reached a duration at which the amount of cAMP that decayed during a burst on side B was as great as the amount that accumulated in response to the presence of reinforcement during a burst on side A. Thus, during training, the amount of conditioning, or the increase in the proportion of time spent producing the operant response, Output A, increased and then stabilized at a new, conditioned level.

3.2. Random Reinforcement Paradigm

In order to demonstrate that the conditioning observed during training depended on the contingency between the occurrence of the operant behavior and the delivery of reinforcement, we introduced a random reinforcement procedure whereby reinforcement was delivered during the training period, but its delivery was not specifically correlated with the behavior of the network (Figure 5b). In these simulations, the number of reinforcement periods was the same as the number during contingent training, and the duration of each period corresponded to the duration of a period of reinforcement in the contingent simulations. Only the timing of the reinforcements was varied randomly. The results of this procedure are compared with those of contingent training in Figure 5c. In contrast to contingent training, when reinforcement was presented randomly during training, there was no significant conditioning of the network. During a random reinforcement simulation, reinforcement was sometimes delivered while AE_A was active and sometimes delivered while AE_B was active. Therefore, a similar amount of cAMP was produced in both AEs, both AE-to-MN connections were facilitated to a comparable degree, feedback to both neurons of the central pattern generator increased, and bursts on both sides of the network increased in duration. However, since, on average, both sides were equally facilitated, there was no change in the relative amount of time the network spent producing either output, A or B (i.e., there was no conditioning). Thus, the network was able to simulate the defining feature of operant conditioning, a change in the amount of time spent producing an output that depended upon the contin-

gency between the occurrence of that output and the delivery of reinforcement. Operant conditioning appeared to be a robust feature of the network. A limited examination of the parameter space, including variation of $\bar{G}_{PG,Ca,V}$, $\bar{G}_{PG,syn}$, T_{FB}, and $K_{PG,UC}$, indicated that while the patterned activity of the network varied over a wide range, operant conditioning was preserved as long as the oscillatory pattern remained.

3.3. Extinction and Reversal of the Contingency

The ability of the network to simulate other features of operant conditioning was also examined. One feature of operant conditioning is that it extinguishes or decays if reinforcement of the operant behavior is discontinued. Accordingly, in our model, when contingent was followed by extinction training (no reinforcement), there was decay of the conditioning toward baseline level (Figure 7). This extinction resulted from the gradual decay of cAMP in the AEs. Due to the kinetics of cAMP synthesis and decay, extinction was slow relative to the acquisition of conditioning, and the conditioning that occurred during the 40 min of contingent training did not completely extinguish during a subsequent 80 min period of extinction training. In *Aplysia*, as in the model, it appears that acquisition of a conditioned response is more rapid than the extinction of that response (Cook & Carew, 1986).

If instead of removing reinforcement, the contingency was reversed during the second training period (reinforcement was delivered when activity in MN_B exceeded activity in MN_A), the reduction of the portion of time spent producing the operant response, Output A, was accelerated. Conditioning was even reduced to below baseline level (Figure 7), due to the associative enhancement of the AE_B-to-MN_B synapse, which tended to increase the relative amount of time spent producing Output B. Similar effects of reversed contingency training were also observed in operant conditioning of head-waving in *Aplysia* (Cook & Carew, 1986).

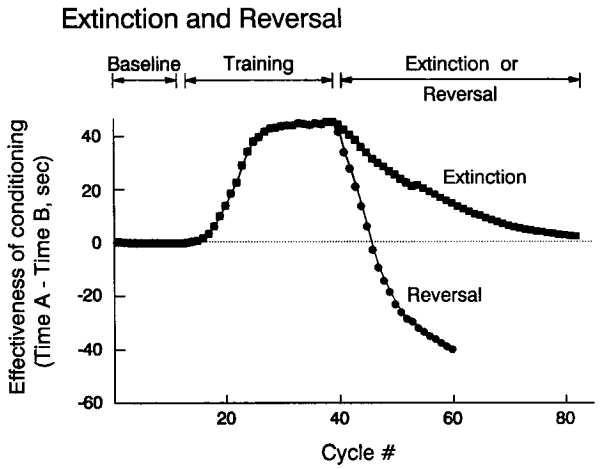

FIGURE 7. Extinction and Reversed Contingency. A 40 min period of contingent training is followed by more than 80 min of either extinction or reversed contingency training. When reinforcement is discontinued during extinction, there is a gradual reduction in the duration of activity in MN_A. When the contingency is reversed (reinforcement is delivered when MN_A is inactive and MN_B is active), the reduction of the portion of time spent producing Output A is accelerated.

3.4. Magnitude of Reinforcement

Although the effects of the magnitude of reinforcement on operant conditioning have not been examined in *Aplysia*, behavioral studies in many animals indicate that conditioning often varies as a function of the magnitude of reinforcement (for review, see Bonem & Crossman, 1988). In the model, the magnitude of reinforcement is represented by K_{EC}, the rate of cAMP synthesis produced by reinforcement in the presence of a given level of Ca^{2+} in the AE (see eqn (18)). Operant conditioning was found to vary as a function of K_{EC} (Figure 8). Conditioning occurred at the highest rate in response to the largest values of K_{EC}. This reflects the more rapid accumulation of cAMP and facilitation of synaptic strength in the AE on the reinforced side of the network with reinforcement of a larger magnitude. Thus, the model can simulate the general feature of operant conditioning that more intense reinforcing stimuli produce an accelerated rate of conditioning.

Another effect of increasing the magnitude of reinforcement in the model was a reduction in the level of conditioning that was reached. This occurred because increasing the rate of cAMP synthesis increased the amount of cAMP produced in the AE on the nonreinforced side of the network as the result of residual Ca^{2+} in that cell. In the AE on the reinforced side, however, the asymptotic level of cAMP was always at the ceiling level, so increasing K_{EC} caused it to reach saturation more rapidly, but it did not increase cAMP beyond its already maximum value. Therefore, the duration of bursts on the nonreinforced side of the network was substantially longer after conditioning when K_{EC} was increased, but the asymptotic duration of bursts on the reinforced side was not affected in this way by changes in K_{EC}. Thus, there was an increase in the relative amount of time spent producing the nonreinforced behavior when K_{EC} was increased, and conditioning was reduced. This result differs from that typically reported in empirical studies of vertebrates, thus providing a testable prediction of the model.

3.5. Delay of Reinforcement

In our model, as in most behavioral studies, increasing the delay between the performance of a behavior and the delivery of reinforcement decreased the rate of conditioning (Figure 9). This occurred because the delay

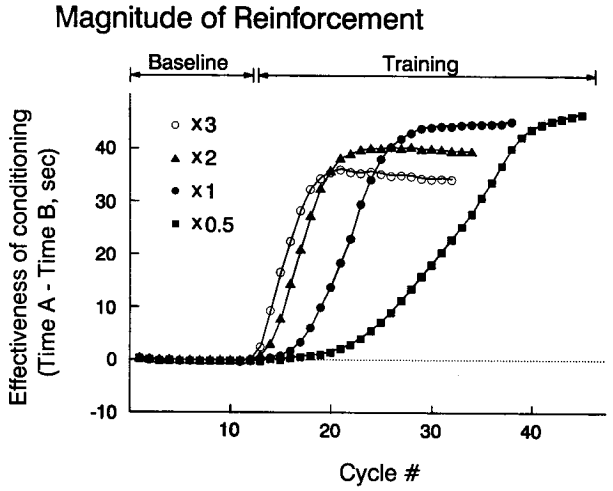

FIGURE 8. Magnitude of Reinforcement. The magnitude of reinforcement was varied by varying K_{EC}, the 'gain' for cAMP production. Conditioning occurs at the highest rate in response to reinforcement of the greatest magnitude.

reduced the amount of time that the reinforcement was present while Ca^{2+} was high in the reinforced AE and low in the nonreinforced AE.

3.6. Sensitivity to Contingency

Most behaviors that exhibit operant conditioning demonstrate a sensitivity to the contingency of reinforcement, the correlation between the occurrence of the operant behavior, and the delivery of reinforcement (Konorski, 1948). If contingency is decreased by delivering reinforcement in the absence of the operant or by not reinforcing each occurrence of the operant, the rate of conditioning is reduced. We simulated both manipulations of contingency. First, extra noncontingent reinforcements were added at random intervals during the contingent training paradigm. This procedure decreased conditioning (Figure 10a). The noncontingent reinforcements contributed to the synthesis of cAMP in both AEs. Since the level of cAMP in the reinforced AE reached the ceiling level during contingent training, cAMP reached the same level whether extra reinforcements were delivered or not. Therefore, the duration of bursts on the reinforced side was approximately six times the length of bursts during baseline after contingent training with or without extra noncontingent reinforcements. However, on the nonreinforced side, since cAMP was not saturated by contingent training, the extra random reinforcements produced additional cAMP, and thus considerably increased the duration of bursts on the nonreinforced side. The result was a decrease in conditioning when contingency was reduced by adding noncontingent presentations of the reinforcement.

The contingency between response and reinforcement was also reduced by changing from a continuous

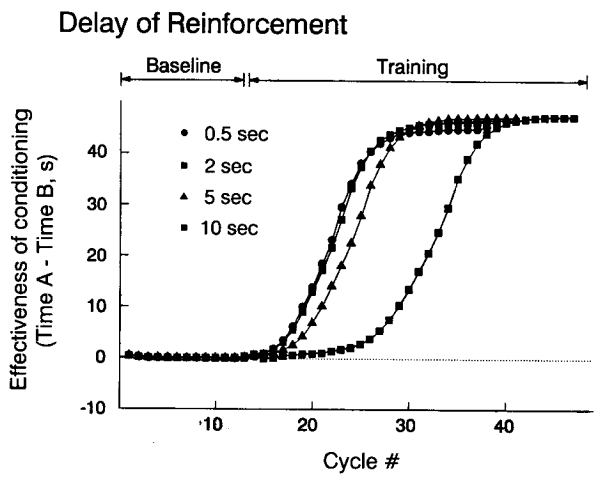

FIGURE 9. Delay of Reinforcement. When the delay between the occurrence of the operant and the delivery of reinforcement is increased, the rate of conditioning is decreased.

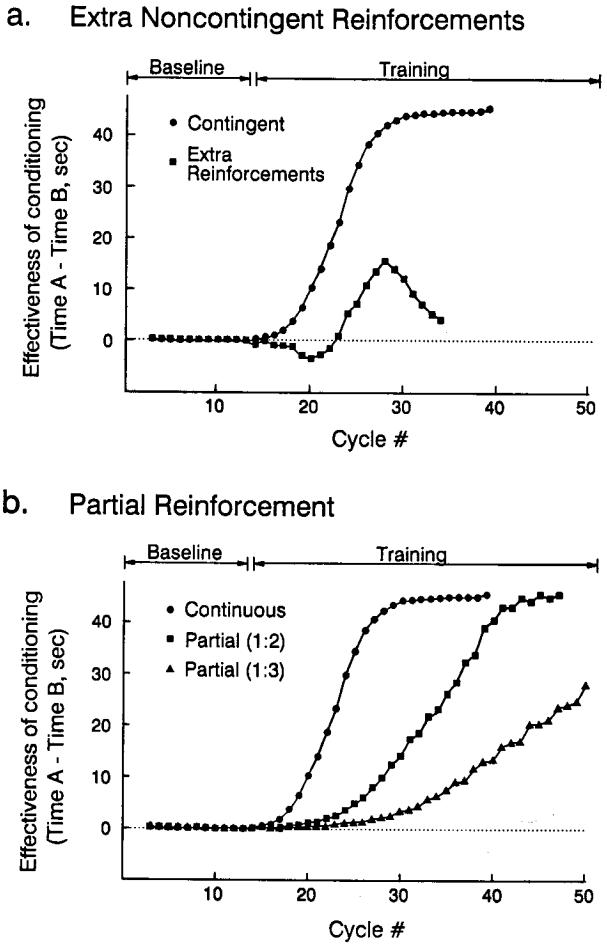

FIGURE 10. Contingency. (a) The delivery of extra, noncontingent reinforcements during contingent training reduces conditioning. (b) A continuous reinforcement schedule (every occurrence of the operant is reinforced) produces more rapid conditioning than a partial reinforcement schedule, which decreases the contingency between response and reinforcement.

reinforcement to a partial reinforcement schedule (i.e., reinforcement was only delivered in response to every other or every third occurrence of the operant behavior; Figure 10b). Partial reinforcement reduced the rate of conditioning because cAMP production was activated less frequently, and therefore cAMP and changes in synaptic strength accumulated more slowly (even for the same number of reinforcements, since there was more time for the decay of cAMP between reinforcements). Thus, the model was able to simulate sensitivity to contingency, a general feature of operant conditioning.

4. DISCUSSION

Our simulations demonstrate that a network with a learning rule derived from a form of associative synaptic plasticity involved in classical conditioning can simulate behavioral data on operant conditioning. Thus, there need not be fundamentally different cellular mechanisms for the two forms of associative learning. Rather, any differences in the neural mechanisms for the two forms of learning may reside in some characteristic feature(s) of the network in which the cellular plasticity is embedded.

To the extent that the circuit and the learning rule in our model reflect features of the actual neural circuitry and plasticity in *Aplysia,* the model predicts several interesting features of operant conditioning of head-waving. First, from the MN traces in Figs. 5 and 6, it is clear that there was an increase in not only the duration but also the amplitude of bursts of activity in the MN corresponding to the reinforced output. These results would predict that some measure of the behavior other than its duration would increase during conditioning. One possibility is that the strength of a muscle contraction that contributes to execution of the reinforced behavior would increase. Indeed, when individual left and right neck muscles of *Aplysia* are subjected to operant conditioning, changes are observed in the differential spike rate in EMG recordings of these muscles (Cook & Carew, 1989b), and such changes are quantitatively related to the magnitude as well as the direction of the head-waving response (Cook & Carew, 1989a). Thus, an output can be changed not only in duration but also in some additional way by the operant training procedure. This feature of our model is a result of the graded inputs and outputs of the MNs and would not emerge if these elements were modeled as simple two-state (ON/OFF) elements.

Second, in our simulations, operant conditioning resulted in a small increase in the absolute duration and amplitude of bursts of activity in the nonreinforced output. This result is consistent with behavioral data using a variety of animal subjects, which indicate that behaviors other than the one that is the target of operant conditioning can also change during training. For example, if a rat is punished for running down an alley, the frequency of flinching, freezing, or withdrawal behaviors may increase, although these behaviors are not being specifically conditioned (Fowler & Miller, 1963). In addition, the presentation of reinforcers, in particular negative reinforcers, can lead to changes in the behavior patterns of subjects, even in the absence of any contingency between their behavior and the delivery of the reinforcer. For example, animals exposed to inescapable shock become inactive (Anisman, deCatanzaro, & Remington, 1978). Our model also demonstrated changes in response to random presentations of reinforcement during control simulations. In our model, changes in outputs that were not contingently reinforced resulted from the interaction of the diffuse modulatory system with residual or 'coincidental' Ca^{2+} in the AE controlling the nonreinforced behavior. These features of conditioning have not yet been examined in *Aplysia;* thus, they represent an important subject for future study.

An important aspect of any model is the way in which its global properties emerge from the interaction of the cellular properties of the individual components of the network and network properties such as connectivity. Our model exhibits several general features of operant conditioning. A number of these result from the specific cellular properties of the AEs. For example, extinction in our model results from the decay of cAMP within the AEs, which causes a return to the baseline values of AE-to-MN synaptic strength and, hence, burst duration. However, other features of the model depend upon an interaction of cellular and circuit properties. The sensitivity to the decreased contingency produced by extra noncontingent presentations of the reinforcement would not occur without the mutual inhibition of the two PGs. Thus, properties of the network as well as cellular properties such as the associative plasticity rule contribute to the overall behavior of the model.

Our simulations illustrate plausible mechanisms by which a number of features of operant conditioning could emerge from a very simple neural network and plasticity rule. This does not mean that other circuits could not produce many of the same features. For example, we chose to incorporate the activity-dependent neuromodulation learning rule into neurons interposed between the CPG and the MNs. This had the advantage of separating, to some extent, the associativity function from other functions of the network (e.g., pattern generation, output, feedback). However, activity-dependent neuromodulation could also have been incorporated into the CPG or the MNs. There exists considerable evidence that these other sites might be important loci of plasticity contributing to conditioning in invertebrates. For example, studies of the conditioning of leg positioning in locust suggest that the motor neurons are a potential site for the associative plasticity involved in this instance of operant conditioning (Hoyle, 1982).

Plasticity at this site would have certain consequences, in particular a loss of specificity, in that all behaviors controlled by the motor neurons, not just the one being conditioned, would be altered by training. In *Aplysia,* for example, if the neck motor neurons were the site of plasticity for the operant conditioning of headwaving, then other behaviors controlled by the neck motor neurons, such as withdrawal of the head, would also be altered by the conditioning of head-waving. There is also evidence that CPGs may contain plastic elements (Getting & Dekin, 1985). Thus, different types of neural elements may be the locus of associative plasticity in different circuits, and an interesting question for future studies is the extent to which the locus of plasticity may determine the features of learning that a particular circuit can support.

REFERENCES

Abrams, T. W., & Kandel, E. R. (1988). Is contiguity detection in classical conditioning a system or cellular property? Learning in *Aplysia* suggests a possible molecular site. *Trends in Neurosciences,* **11,** 128–136.

Anisman, H., deCatanzaro, D., & Remington, G. (1978). Escape performance following exposure to inescapable shock: Deficits in motor response maintenance. *Journal of Experimental Psychology: Animal Behavior Processes,* **4,** 197–218.

Baxter, D. A., Raymond, J. L., Buonomano, D. V., & Byrne, J. H. (1989). Operant conditioning can be simulated by small networks of neuron-like adaptive elements. *Society for Neuroscience Abstracts,* **15,** 1263.

Baxter, D. A., Raymond, J. L., Buonomano, D. V., Cook, D. G., Kuenzi, F. M., Carew, T. J., & Byrne, J. H. (1991). Empirically derived adaptive elements and networks simulate associative learning. In M. L. Commons, S. Grossberg, & J. E. R. Staddon (Eds.), *Neural network models of conditioning and action* (Volume XII Quantitative analyses of behavior) (pp. 13–52). Hillsdale, NJ: Lawrence Erlbaum and Associates.

Bonem, M., & Crossman, E. K. (1988). Elucidating the effects of reinforcement magnitude. *Psychological Bulletin,* **104,** 348–362.

Buonomano, D. V., Baxter, D. A., & Byrne, J. H. (1990). Small networks of empirically derived adaptive elements simulate some higher-order features of classical conditioning. *Neural Networks,* **3,** 507–523.

Buonomano, D. V., & Byrne, J. H. (1990). Long-term synaptic changes produced by a cellular analog of classical conditioning in *Aplysia. Science,* **249,** 420–423.

Byrne, J. H. (1985). Neural and molecular mechanisms underlying information storage in *Aplysia:* Implications for learning and memory. *Trends in Neurosciences,* **8,** 478–482.

Byrne, J. H. (1987). Cellular analysis of associative learning. *Physiological Reviews,* **67,** 329–439.

Byrne, J. H., Baxter, D. A., Buonomano, D. V., & Raymond, J. L. (1991). Neuronal and network determinants of simple higher-order features of associative learning: Experimental and modeling approaches. *Cold Spring Harbor Symposia on Quantitative Biology,* **55,** 175–186.

Calabrese, R. L., & Peterson, E. L. (1983). Neural control of heartbeat in the leech, *Hirudo medicinalis.* In A. Roberts & B. Roberts (Eds.), *Neural origin of rhythmic movements* (Volume 37 Symposia of the Society for Experimental Biology) (pp. 195–221). New York: Cambridge University Press.

Cook, D. G., & Carew, T. J. (1986). Operant conditioning of headwaving in *Aplysia. Proceedings of the National Academy of Sciences of the United States of America,* **83,** 1120–1124.

Cook, D. G., & Carew, T. J. (1989a). Operant conditioning of headwaving in *Aplysia* I: Identified muscles involved in the operant response. *Journal of Neuroscience,* **9,** 3097–3106.

Cook, D. G., & Carew, T. J. (1989b). Operant conditioning of headwaving in *Aplysia* II: Contingent modification of electromyographic activity in identified muscles. *Journal of Neuroscience,* **9,** 3107–3114.

Cook, D. G., & Carew, T. J. (1989c). Operant conditioning of headwaving in *Aplysia* III: Cellular analysis of possible reinforcement pathways. *Journal of Neuroscience,* **9,** 3115–3122.

Eckert, R., & Tillotson, D. (1981). Calcium-mediated inactivation of the calcium conductance in caesium-loaded giant neurones of *Aplysia. Journal of Physiology (London),* **314,** 265–280.

Fowler, H., & Miller, N. E. (1963). Facilitation and inhibition of runway performance by hind- and forepaw shock of various intensities. *Journal of Comparative and Physiological Psychology,* **56,** 801–805.

Getting, P. A. (1981). Mechanisms of pattern generation underlying swimming in *Tritonia.* I. Neuronal network formed by monosynaptic connections. *Journal of Neurophysiology,* **46,** 65–79.

Getting, P. A. (1989). Emerging principles governing the operation of neural networks. *Annual Review of Neuroscience,* **12,** 185–204.

Getting, P. A., & Dekin, M. S. (1985). Mechanisms of pattern generation underlying swimming in *Tritonia.* IV. Gating of a central pattern generator. *Journal of Neurophysiology,* **53,** 466–480.

Gingrich, K. J., & Byrne, J. H. (1985). Simulation of synaptic depression, posttetanic potentiation, and presynaptic facilitation of synaptic potentials from sensory neurons mediating the gill-withdrawal reflex in *Aplysia. Journal of Neurophysiology,* **53,** 652–669.

Gingrich, K. J., & Byrne, J. H. (1987). Single-cell model for associative learning. *Journal of Neurophysiology,* **57,** 1705–1715.

Gluck, M. A., & Thompson, R. F. (1987). Modeling the neural substrates of associative learning and memory: A computational approach. *Psychological Review,* **94,** 176–191.

Grossberg, S. (1971). On the dynamics of operant conditioning. *Journal of Theoretical Biology,* **33,** 225–255.

Hawkins, R. D. (1989). A simple circuit model for higher-order features of classical conditioning. In J. H. Byrne & W. O. Berry (Eds.), *Neural models of plasticity* (pp. 73–93). San Diego, CA: Academic Press.

Hawkins, R. D., Abrams, T. W., Carew, T. J., & Kandel, E. R. (1983). A cellular mechanism of classical conditioning in *Aplysia:* Activity-dependent amplification of presynaptic facilitation. *Science,* **219,** 400–405.

Hawkins, R. D., & Kandel, E. R. (1984). Is there a cell-biological alphabet for simple forms of learning? *Psychological Review,* **91,** 376–391.

Hoyle, G. (1982). Cellular basis of operant conditioning of leg positioning. In D. Carpenter (Ed.), *Conditioning: Representation of involved neural functions* (pp. 3–25). New York: Plenum.

Konorski, J. (1948). *Conditioned reflexes and neuron organization.* New York: Cambridge University Press.

Kramer, R. H., & Zucker, R. S. (1985). Calcium-induced inactivation of calcium current causes the inter-burst hyperpolarizations of *Aplysia* bursting neurones. *Journal of Physiology (London),* **362,** 131–160.

Oyama, Y., Akaike, N., & Nishi, K. (1986). Persistent calcium inward current in internally perfused snail neuron. *Cellular and Molecular Neurobiology,* **6,** 71–85.

Pavlov, I. P. (1927). *Conditioned reflexes.* London: Oxford University Press.

Rescorla, R. A. (1987). A Pavlovian analysis of goal-directed behavior. *American Psychologist,* **42,** 119–129.

Selverston, A. I., Miller, J. P., & Wadepuhl, M. (1983). Cooperative mechanisms for the production of rhythmic movements. In A.

Roberts & B. Roberts (Eds.), *Neural origin of rhythmic movements* (Volume 37 Symposia of the Society for Experimental Biology) (pp. 55–58). New York: Cambridge University Press.

Skinner, B. F. (1938). *The behavior of organisms.* New York: Appleton-Century.

Thorndike, E. L. (1911). *Animal intelligence: Experimental studies.* New York: Macmillan.

Tully, T., & Quinn, W. G. (1985). Classical conditioning and retention in normal and mutant *Drosophila melanogaster. Journal of Comparative Physiology A,* **157,** 263–277.

Walters, E. T., & Byrne, J. H. (1983). Associative conditioning of single sensory neurons suggests a cellular mechanism for learning. *Science,* **219,** 405–408.

APPENDIX

Adaptive Elements (AEs)

The equations used for the adaptive elements are presented below. For additional details see Gingrich and Byrne (1985, 1987).

Dynamics of Ca^{2+}

$$I_{AE,Ca} = A \cdot B \cdot K_C, \tag{A1}$$

$$A = 1 - \exp(-t_1/T_A), \tag{A2}$$

$$B = C \cdot \exp(-t_1/T_I), \tag{A3}$$

$$C = 1 - (1 - B') \cdot \exp(-t_2/T_{\mathrm{REC}}), \tag{A4}$$

$$F_{UC} = K_U/(1 + M_U/C_{AE,Ca}^2), \tag{A5}$$

$$F_{DC} = C_{AE,Ca} \cdot K_D, \tag{A6}$$

$$\frac{dC_{AE,Ca}}{dt} = \frac{(I_{AE,Ca} - F_{UC} - F_{DC})}{V_C}. \tag{A7}$$

Dynamics of Transmitter Mobilization

$$F_D = (C_S - C_R) \cdot K_{VD}, \tag{A8}$$

$$F_C = \left(PVM_S + \frac{K_F}{1 + M_F/C_{AE,Ca}^{\mathrm{Nf}}}\right), \tag{A9}$$

$$\frac{dPVM_S}{dt} = \left(\frac{K_S}{(1 + M_S/C_{AE,Ca}^{\mathrm{Ns}})} - PVM_S\right) \cdot \frac{1}{T_S}, \tag{A10}$$

$$F_{cAMP} = K_{FC} \cdot C_{cAMP}, \tag{A11}$$

$$\frac{dC_R}{dt} = (F_{cAMP} + F_C + F_D - T_R) \cdot (1/V_R). \tag{A12}$$

Dynamics of cAMP

In the absence of activity in the FN:

$$\frac{dC_{cAMP}}{dt} = (-C_{cAMP}/T_{cAMP}). \tag{A13}$$

In the presence of activity in the FN:

$$\frac{dC_{cAMP}}{dt} = (-C_{cAMP}/T_{cAMP}) + (K_{EC} \cdot C_{AE,Ca}). \tag{A14}$$

Release of Transmitter

$$\text{spike duration} = 0.003 + (K_{DC} \cdot C_{cAMP}), \tag{A15}$$

$$T_R = C_R \cdot V_R \cdot I_{Ca} \cdot K_R. \tag{A16}$$

Values and Definitions of Constants

C_s	100	concentration of transmitter in storage pool
$C_{\max}$	2400	cAMP ceiling
K_c	1.0	constant for Ca^{2+} current
K_D	0.34	diffusion constant for Ca^{2+}
K_{DC}	$1.5 \cdot 10^{-5}$	constant for spike duration
K_{EC}	50	constant for Ca^{2+}-dependent synthesis of cAMP
K_F	21.0	maximal rate of fast mobilization
K_{FC}	$2 \cdot 10^{-4}$	constant for cAMP-dependent mobilization
K_R	1.0	constant for transmitter release
K_S	35.0	maximal rate of slow mobilization
K_U	2907	constant for Ca^{2+} uptake
K_{VD}	0.001	constant for diffusion of transmitter
M_F	0.0008	concentration constant for fast mobilization
M_S	0.075	concentration constant for slow mobilization
M_U	790.0	concentration constant for Ca^{2+} uptake
N_f	2.83	Hill coefficient for fast mobilization
N_S	1.75	Hill coefficient for slow mobilization
T_A	0.001	time constant for activation of Ca^{2+} channel
T_{cAMP}	900	time constant of cAMP
T_I	0.44	time constant for inactivation of Ca^{2+} channel
T_{REC}	0.01	time constant for recovery from inactivation of Ca^{2+} channel
T_S	213.0	time constant for slow mobilization
V_C	2.15	volume of Ca^{2+} compartment
V_R	1.0	volume of releasable pool

Initial Values and Definitions of Variables

A	0	activation of Ca^{2+} channel
B	1	inactivation of Ca^{2+} channel during spike
B'	1	value of B at end of a spike
C	1	recovery from inactivation of Ca^{2+} channel
$C_{AE,Ca}$	0	concentration of Ca^{2+}
C_{cAMP}	0	concentration of cAMP
C_R	500	concentration of transmitter in releasable pool
F_C	0	Ca^{2+}-dependent mobilization
F_{cAMP}	0	cAMP-dependent mobilization
F_D	0	diffusion of transmitter
F_{DC}	0	diffusion of Ca^{2+}
F_{UC}	0	uptake of Ca^{2+}
$I_{AE,Ca}$	0	Ca^{2+} current
PVM_S	0	potential for mobilization
t_1	0	time after beginning of spike
t_2	0	time after last spike
T_R	0	release of transmitter

NEURONS OF THE CENTRAL PATTERN GENERATOR (PGs)

Values and Definitions of Constants

C_m	$1.3 \cdot 10^{-3}$	membrane capacitance
E_{Ca}	120	equilibrium potential for Ca^{2+}
E_K	−75	equilibrium potential for K^+
$\bar{G}_{PG,ahp}$	0.5	maximum conductance for $I_{PG,ahp}$
$\bar{G}_{PG,Ca}$	0.002	maximum conductance for $I_{PG,Ca}$
$\bar{G}_{PG,Ca,V}$	0.625	maximum conductance for $I_{PG,Ca,V}$
$\bar{G}_{PG,syn}$	0.25	maximum conductance for $I_{PG,syn}$
K_{FB}	0.36	feedback constant for modulation of $I_{PG,Ca,V}$

$K_{PG,DC}$	0.054	diffusion constant for Ca^{2+}
$K_{PG,UC}$	0.54	uptake constant for Ca^{2+}
$T_{PG,ahp}$	0.011	time constant for activation and inactivation of $I_{PG,ahp}$
$T_{PG,Ca,V}$	$5.0 \cdot 10^{-4}$	time constant for activation and inactivation of $I_{PG,Ca,V}$
$T_{PG,syn}$	0.075	time constant for activation and inactivation of $I_{PG,syn}$
V_{PG}	2.15	volume of cytosol

Initial Values of Variables

The initial value of all variables is zero, with the exception of the following:

$V_m(PG_A)$	−60	membrane potential in PG_A
$V_m(PG_B)$	−70	membrane potential in PG_B

MOTOR NEURONS (MNs)

Values and Definitions of Constants

T_{FB}	1.0	time constant for feedback
T_M	0.1	time constant for response of MN to transmitter

Initial Values of Variables

AMN	0	activation level
F	0	feedback

The model was implemented with a program written in FORTRAN using the Euler method of integration with a uniform integration step size of $2.0 \cdot 10^{-4}$ sec. All times and time constants are given in seconds.